



## NO<sub>x</sub>-conversion on Porous LSF15-CGO10 Cell Stacks with KNO<sub>3</sub> or K<sub>2</sub>O Impregnation

Traulsen, Marie Lund; Bræstrup, Frantz Radzik; Kammer Hansen, Kent

*Published in:*  
Journal of Solid State Electrochemistry

*Link to article, DOI:*  
[10.1007/s10008-012-1684-9](https://doi.org/10.1007/s10008-012-1684-9)

*Publication date:*  
2012

[Link back to DTU Orbit](#)

*Citation (APA):*  
Traulsen, M. L., Bræstrup, F. R., & Kammer Hansen, K. (2012). NO<sub>x</sub>-conversion on Porous LSF15-CGO10 Cell Stacks with KNO<sub>3</sub> or K<sub>2</sub>O Impregnation. *Journal of Solid State Electrochemistry*, 16, 2651–2660.  
<https://doi.org/10.1007/s10008-012-1684-9>

---

### General rights

Copyright and moral rights for the publications made accessible in the public portal are retained by the authors and/or other copyright owners and it is a condition of accessing publications that users recognise and abide by the legal requirements associated with these rights.

- Users may download and print one copy of any publication from the public portal for the purpose of private study or research.
- You may not further distribute the material or use it for any profit-making activity or commercial gain
- You may freely distribute the URL identifying the publication in the public portal

If you believe that this document breaches copyright please contact us providing details, and we will remove access to the work immediately and investigate your claim.

# NO<sub>x</sub>-conversion on Porous LSF15-CGO10 Cell Stacks with KNO<sub>3</sub> or K<sub>2</sub>O Impregnation

M. L. Traulsen

F. Bræstrup

K. Kammer Hansen

Fuel Cells and Solid State Chemistry Division, Risø National Laboratory for Sustainable Energy,  
Technical University of Denmark, DK-4000 Roskilde, Denmark

## Abstract

In the present work it was investigated how addition of KNO<sub>3</sub> or K<sub>2</sub>O affected the NO<sub>x</sub> conversion on LSF15-CGO10 (La<sub>0.85</sub>Sr<sub>0.15</sub>FeO<sub>3</sub>-Ce<sub>0.9</sub>Gd<sub>0.1</sub>O<sub>1.95</sub>) composite electrodes during polarisation. The LSF15-CGO10 electrodes were part of a porous 11-layer cell stack with alternating layers of LSF15-CGO10 electrodes and CGO10 electrolyte. The KNO<sub>3</sub> was added to the electrodes by impregnation, and kept either as KNO<sub>3</sub> in the electrode or thermally decomposed into K<sub>2</sub>O before testing. The cell stacks were tested in the temperature range 300-500 °C in 1000 ppm NO, 10% O<sub>2</sub> and 1000 ppm NO + 10% O<sub>2</sub>. During testing the cells were characterized by electrochemical impedance spectroscopy (EIS) and the NO conversion was measured during polarization at -3 V for 2 h. The concentration of NO and NO<sub>2</sub> was monitored by a chemiluminescence detector, while the concentration of O<sub>2</sub>, N<sub>2</sub> and N<sub>2</sub>O was detected on a mass spectrometer. A significant effect of impregnation with KNO<sub>3</sub> or K<sub>2</sub>O on the NO<sub>x</sub> conversion was observed. In 1000 ppm NO both impregnations caused an increased conversion of NO into N<sub>2</sub> in the temperature range 300-400 °C with a current efficiency up to 73%. In 1000 ppm NO + 10% O<sub>2</sub> no formation of N<sub>2</sub> was observed during polarisation, but the impregnations altered the conversion between NO and NO<sub>2</sub> on the electrodes. Both impregnations caused increased degradation of the cell stack, but the exact cause of the degradation has not been identified yet.

**Keywords:** Exhaust gas cleaning, NO<sub>x</sub> removal, NO<sub>x</sub> reduction, deNO<sub>x</sub>, impregnation, LSF

E-mail: [matr@risoe.dtu.dk](mailto:matr@risoe.dtu.dk) Phone +45 21 32 79 37 Fax:+45 46 77 58 58

## Introduction

$\text{NO}_x$  is an air pollutant which has a number of negative effects on human health and the environment, as  $\text{NO}_x$  affects the respiratory system negatively, increase the formation of ozone at ground level, cause formation of acid rain, contribute to smog formation and also act as green house gas [1]. In gasoline vehicles  $\text{NO}_x$  can be removed sufficiently from the exhaust by the Three-Way-Catalyst (TWC), but this catalyst does not work for diesel vehicles due to a higher oxygen content in diesel engine exhaust [2]. For this reason other technologies are used for  $\text{NO}_x$ -removal from diesel engine exhaust; the three most well-known technologies being selective catalytic reduction with urea (urea-SCR), selective catalytic reduction with hydrocarbons (HC-SCR) and the  $\text{NO}_x$ -storage and reduction (NSR) catalyst [2].

An alternative technology under development for  $\text{NO}_x$ -removal is electrochemical de $\text{NO}_x$  [3-5], which compared to the three aforementioned technologies has the advantage no extra reducing agents needs to be supplied, as the NO is reduced by electrons during polarisation. Pancharatnam et al. discovered in 1975 NO can be reduced to  $\text{N}_2$  during polarisation in absence of oxygen [6] and later it was discovered NO can also be reduced during polarisation in the presence of oxygen [7][8], which made electrochemical de $\text{NO}_x$  of interest for cleaning of oxygen containing exhaust gasses.

Since then several studies have been carried within electrochemical de $\text{NO}_x$  [9-15], however the main challenges in the development of electrochemical de $\text{NO}_x$  continues to be to achieve a sufficiently high activity and selectivity [5]. In this work it is attempted to improve the selectivity and activity of the LSF15-CGO10 composite electrodes for electrochemical de $\text{NO}_x$  by adding a  $\text{NO}_x$ -storage compound, as known from NSR catalysis, to the electrodes.

The addition of the NO<sub>x</sub>-storage compound to the electrodes is expected to improve the NO<sub>x</sub> conversion by concentrating the NO<sub>x</sub> in the form of nitrates on the electrode surface. Promising results has so far been achieved with combining electrochemical deNO<sub>x</sub> and a NO<sub>x</sub> storage compound by Nagao et al. [13] and Hamamoto et al. [14] however in both cases the electrode contained platinum. Two important questions arises when adding af NO<sub>x</sub> storage compound to the electrodes used in this work: 1) As no platinum is present in the electrodes, will the electrode material itself be able to oxidize NO to NO<sub>2</sub>, as this step needs to precede the formation of nitrate on the storage compound? 2) How will the presence of a NO<sub>x</sub>-storage compound alter the electrode processes?

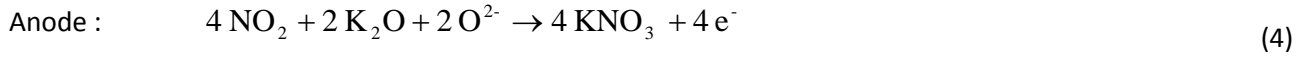
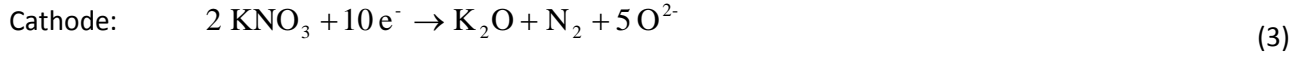
With respect to question 1), Werchmeister et al. has shown electrochemical reduction of NO on LSM(La<sub>1-x</sub>Sr<sub>x</sub>MnO<sub>3</sub>)-CGO, LSF-CGO and LSCF(La<sub>1-x</sub>Sr<sub>x</sub>Co<sub>1-y</sub>Fe<sub>y</sub>O<sub>3-δ</sub>)-CGO electrodes was preceded by catalytically formation of NO<sub>2</sub> [15, 16]. For this reason formation of nitrates for NO<sub>x</sub>-storage is likely possible, even when platinum is not present on the electrodes used for electrochemical deNO<sub>x</sub>.

Question 2) is not easy to answer but a suggestion can be made for the overall electrode processes, which may be useful to keep in mind during the later interpretation of the results. On a cell without a NO<sub>x</sub>-storage compound the expected electrode processes for electrochemical reduction of NO is:



Note the equations above state the overall processes and do not take into account any catalytic formation of NO<sub>2</sub>. On the cathode a dominating, competing reaction to the reduction of NO is the reduction of O<sub>2</sub>: O<sub>2</sub> + 4 e<sup>-</sup> → 2 O<sup>2-</sup>.

When a NO<sub>x</sub>-storage compound like K<sub>2</sub>O/KNO<sub>3</sub> is added to the electrodes, one could imagine the electrode processes to become:



However, the formation of KNO<sub>3</sub> is not necessarily an electrochemical process as described in the anode-equation above, but could just be a chemical reaction:  $4 \text{ NO}_2 + 2 \text{ K}_2\text{O} + \text{O}_2 \rightarrow 4 \text{ KNO}_3$  as in conventional NSR catalysis, in that case O<sub>2</sub> could be supplied from oxidation of the O<sup>2-</sup> at the anode or from the surrounding atmosphere. An improved performance for electrochemical deNO<sub>x</sub> could eventually be gained by repeatedly changing the current direction through the cell, and thereby making the electrodes act alternately as cathodes and anodes, as shown by Hibino et al. [17] and Hamamoto et al. [14]. However, such experiments were not made in this work, since the available test-setup did not allow for precise measurements of the effect of alternating polarisation on the gas composition.

In this work three different LSF15-CGO10 cell stacks were tested with respect to conversion of NO<sub>x</sub> in the temperature range 300-500 °C. The stacks were subjected to electrochemical impedance spectroscopy and conversion/polarisation experiments while the gas composition was monitored by a mass spectrometer (MS) and a chemiluminiscense detector (CLD). The cell stacks differed from each other in the way they were impregnated: one stack had no impregnation, one stack was impregnated with KNO<sub>3</sub> and one stack was impregnated with K<sub>2</sub>O. LSF was chosen as electrode material, since LSF as a mixed conductor [18][19] has been evaluated to be a promising material for intermediate temperate solid oxide electrodes [20] while CGO was chosen as an electrolyte, as CGO has superior oxygen ion-conductivity below 600 °C when compared to yttria stabilized zirconia [21]. KNO<sub>3</sub>/K<sub>2</sub>O was chosen for impregnation, as potassium is known to act both as a NO<sub>x</sub>-

storage compound [22] and also to improve simultaneous NO<sub>x</sub> and soot removal [23, 24], the latter being of interest for future development of the electrochemical deNO<sub>x</sub> technique. With respect to the development of the electrochemical deNO<sub>x</sub> technique it must be emphasized, the work presented in this paper is at the very early stage of the development process, and only deals with investigated materials ability to electrochemically convert NO<sub>x</sub> in model atmospheres containing only NO<sub>x</sub>, O<sub>2</sub> and Ar, even though real diesel exhaust also contains significant amounts of CO<sub>2</sub> and H<sub>2</sub>O [25]. The presence of CO<sub>2</sub> and H<sub>2</sub>O may influence the performance and degradation of the electrochemical deNO<sub>x</sub> electrodes. In that context it is important that formation of stable carbonate species does not appear to be a problem on potassium containing catalysts in the presence of NO<sub>x</sub> [22, 26], while the influence of H<sub>2</sub>O on the potassium impregnated LSF15-CGO10 electrodes is not clear and will have to be investigated in the future.

## **Experimental**

### *Fabrication of porous cell stacks*

The cell stacks tested in this work were ceramic, porous cell stacks consisting of 11 alternating layers of electrode and electrolyte. The porous stack design was chosen for this work, as the large contact area between gas and cell in this design makes it easy to measure the NO-conversion.

The electrode layers in the porous cell stacks were a LSF15-CGO10 composite with 65 wt% LSF15 and 35 wt% CGO10. The LSF had been synthesized in house by the glycine-nitrate combustion synthesis [27] from nitrate solutions supplied by Alfa Aesar. The LSF15 was synthesized with the exact composition La<sub>0.84</sub>Sr<sub>0.149</sub>FeO<sub>3</sub>. The CGO10 was supplied by Rhodia. For the fabrication of the composite electrode the LSF15 and CGO10 were mixed with solvent, binder, dispersant and poreformer (graphite), ball milled and subsequently tapecasted. For more detailed information on the tapecasting procedure see He et al. [28]. The porous CGO electrolyte was tapecasted like the electrode tape and afterwards the green electrode and electrolyte tapes were laminated

together with 6 electrode layers alternating with 5 electrolyte layers. Round cell stacks with a diameter of 18 mm were stamped out of the green laminated tapes and thereafter sintered at 1250 °C. During the sintering the graphite poreformer was burned off leaving behind the pores in the stack. Before testing a porous Au current collector was applied to the cell stack by painting the outer electrodes with a gold paste containing 20 wt% carbon, and subsequent heat the cell stack to 800 °C to decompose the graphite. An image of the 11-layer cell stack with the porous current collector is shown in Fig. 1.

### *Impregnation*

For impregnation of the cell stacks an aqueous solution of 3.1 M  $\text{KNO}_3$  (Alfa Aesar) was prepared. The solution also contained 10 wt% P123 (BASF) with respect to the water. The impregnation was made by covering the cell stack with impregnation solution and then placing the cell stack in a vacuum chamber and evacuate to a pressure below 0.1 mbar for approximately 15 s. Excess impregnation solution was wiped of the surface of the cell stack, and thereafter the cells were heated to 350 °C to decompose the P123. The cell impregnated with  $\text{K}_2\text{O}$  was prepared in exactly the same way, apart from the cell was heated to 700 °C to decompose the  $\text{KNO}_3$  into  $\text{K}_2\text{O}$ .

### *Test-setup*

For electrochemical cell testing the stack was mounted in between two alumina tubes, which contained channels for the gas flow and measurement probes for the electrochemical characterization. The cell and the alumina tubes were inclosed in a quartz tube and mounted vertically in a furnace. A sketch of the set-up is shown in Fig. 2.

### *Electrochemical characterization*

A Gamry reference 600 potentiostat was used for the electrochemical characterization of the cell stack.

Electrochemical impedance spectra were recorded in the frequency range 1 MHz to 0.001 Hz with 36 mV rms amplitude and 6 points pr. decade. For the conversion experiments the cell stack was first kept at Open Circuit Voltage (OCV) for 2 h, then polarized at -3 V for 2 h, and afterwards left at OCV for 2 h again. The electrochemical characterization was made first at 300 °C, and then repeated for each 50 °C until 500 °C was reached. After this the cell was cooled down to 300 °C, one EIS spectrum was recorded to evaluate the degradation during the cell test, and thereafter the test was finished.

### *Conversion measurements*

The cell stack was supplied with NO, O<sub>2</sub> and Ar from Brooks mass flow controllers. The conversion measurements were made in 1000 ppm NO and 1000 ppm NO +10% O<sub>2</sub> in both cases with balance Ar. These concentrations of NO and O<sub>2</sub> were chosen as they resemble the concentrations which may be found in the exhaust from a diesel car [25]. The NO and NO<sub>2</sub> content in the gas stream from the cell was monitored by a chemiluminescence detector Model 42i High Level from Thermo Scientific; while the N<sub>2</sub>, N<sub>2</sub>O and O<sub>2</sub> concentration was monitored by a mass spectrometer from Pfeiffer Vacuum, type Omnistar GSD 301.

### *Scanning Electron Microscopy*

The cell stacks were examined in a Zeiss Supra 35 scanning electron microscope equipped with a field emission gun. SEM images were recorded in two ways: In order to obtain high magnification images of the electrode microstructure images were recorded with the in-lens detector and 3 keV acceleration voltage on cells just broken and put directly into the microscope. To get more overall images of the cell stacks and the different layers in the stacks a part of each stack was mounted in epoxy, polished and carbon coated prior to the microscopy investigation.



## Results and Discussion

### *Microstructure of electrodes before and after testing*

Fig. 3 shows the microstructure of the electrodes in the three different tested cell stacks. In the non-impregnated cell stack (Fig. 3a) all the electrode grains appear to have a well-defined shape and very smooth surfaces. In the  $\text{KNO}_3$  impregnated cell stack (Fig. 3b) the infiltrated  $\text{KNO}_3$  is present around in the electrode structure as lumps with a porous looking surface. The porous looking  $\text{KNO}_3$ -surface is likely due to interaction between the electron-beam and the  $\text{KNO}_3$ , as focusing the electron beam on the  $\text{KNO}_3$  altered the look of the  $\text{KNO}_3$  lumps. Fig. 3b also shows even though the  $\text{KNO}_3$  is present as big lumps in the electrode, there is still open porosity left for the gas to pass through. The electrode of the cell stack which had been impregnated with  $\text{KNO}_3$  and subsequent heated to 700 °C to decompose the  $\text{KNO}_3$  into  $\text{K}_2\text{O}$  is shown in Fig. 3c. In the electrode  $\text{KNO}_3$  lumps are observed together with other irregular shaped  $\text{K}_2\text{O}$  grains.

Samples from before and after electrochemical cell testing were mounted in epoxy and examined in the microscope to obtain information about changes in the electrode microstructure during testing. No change due to the testing was observed on the non-impregnated sample. However, both the  $\text{KNO}_3$  impregnated sample and the  $\text{K}_2\text{O}$  impregnated sample showed a significant change in microstructure after the testing. The change in microstructure is best described as the grain size had been reduced and/or the attachments between the electrode grains decreased. The change in microstructure was most pronounced in the outer electrodes of the cell stack and is illustrated in Fig. 4 for the  $\text{KNO}_3$  impregnated sample.

### *Conversion and Current efficiency*

No purely catalytic effect of the  $\text{KNO}_3$  or  $\text{K}_2\text{O}$  impregnation was detected, as no difference between the impregnated and non-impregnated cell stacks was observed in the outlet NO concentration, when the stacks before polarisation were flushed in either 1000 ppm NO or 1000 ppm NO + 10%  $\text{O}_2$ .

In 1000 ppm NO zero conversion of  $\text{NO}_x$  into  $\text{N}_2$  during 3 V polarisation for 2 h was observed at 300 and 350 °C on the non-impregnated cell stack. However, from 400 °C to 500 °C the conversion into  $\text{N}_2$  increased from 4% to 43%, see Table 1. On the impregnated cell stacks  $\text{NO}_x$  conversion in the range 2-17% was observed at 300-350 °C, which means higher  $\text{NO}_x$  conversion was observed at low temperatures on the impregnated cell stacks compared to the non-impregnated cell stack. In contradiction to this the  $\text{NO}_x$  conversion was lower on the impregnated cell stacks compared to the non-impregnated sample at higher temperatures. A significant decrease in  $\text{NO}_x$  conversion on the  $\text{KNO}_3$  impregnated sample was observed from 350 °C to 400 °.

The current efficiency during the 2 h polarisation was calculated according to Eq. (5):

$$\text{Current efficiency} = \frac{I_{\text{N}_2}}{I_{\text{applied}}} \cdot 100\% \quad (5)$$

- where  $I_{\text{N}_2}$  is the current corresponding to the reduction of NO into the  $\text{N}_2$ , which was detected by the MS, and  $I_{\text{applied}}$  is the current applied on the cell during the polarisation. In Table 2 the current efficiencies in the different tests are stated for the atmosphere with 1000 ppm NO in Ar. It is observed impregnation with  $\text{KNO}_3$  and  $\text{K}_2\text{O}$  increases the current efficiencies in the temperature range 300-400 °C. Improved current efficiency at 500 °C is also observed for the  $\text{K}_2\text{O}$  impregnated sample. The current not used for reduction of NO is used for the competing reduction of  $\text{O}_2$ . The  $\text{O}_2$  likely had been adsorbed on the cell stack during treatment in 10%  $\text{O}_2$  in

between the polarisation experiments or originate from a small leak in the system, as 70 -100 ppm  $O_{2,leak}$  was measured by the MS while the sample was supplied with 1000 ppm NO in Ar.

In addition to conversion into  $N_2$  oxidation of NO into  $NO_2$  takes place during polarisation of the cell stacks in 1000 ppm NO. In Fig. 5 it is illustrated how the conversion into  $NO_2$  is highest at 300-400 °C for the impregnated cell stacks, whereas for the non-impregnated cell stack conversion into  $NO_2$  is only observed in the temperature range 400-500 °C. With respect to the non-impregnated cell stack a decrease in  $O_{2,leak}$  was observed during polarisation/formation of  $NO_2$ . The oxygen balance over the blank cell stack at all temperatures showed a deviation below 15 ppm  $O_2$ , when comparing the concentrations of NO,  $NO_2$  and  $O_{2,leak}$  before and during polarisation. For the impregnated cell stacks the oxygen balance showed in general an excess  $O_2$  concentration during polarisation (up to 100 ppm), indicating previously adsorbed  $O_2$  was released from the cell stack during polarisation.

When oxygen was present in the atmosphere, conversion of  $NO_x$  into  $N_2$  was not observed for any of the samples. It should be noted even though the gas composition when oxygen was present in this article is stated as 1000 ppm NO + 10%  $O_2$  the actual concentration of NO was in the range 700-900 ppm due to the equilibrium  $2 NO + O_2 \rightleftharpoons 2 NO_2$ .

Instead of reduction of  $NO_x$  into  $N_2$  an increased conversion between NO and  $NO_2$  was observed on the samples during polarisation in oxygen containing atmospheres. A significant difference between the cell stack without impregnation and the impregnated stacks was observed: without impregnation NO was formed during polarisation due to conversion of  $NO_2$ , whereas for the samples impregnated with  $KNO_3$  or  $K_2O$   $NO_2$  was formed during polarisation due to conversion of NO. This is clear when Fig. 6 and Fig. 7 are compared, where Fig. 6 shows the change in NO concentration during polarisation and Fig. 7 shows the change in  $NO_2$  during polarisation, in both cases relative to the NO concentration before the samples were polarized. The current

through the cell stacks was in 1-20 mA during the polarisation at -3V for both the non-impregnated and the impregnated cell stacks.

The increased NO conversion due to the presence of potassium observed in this work is in agreement with results reported by Hamamoto et al. [14]. Hamamoto et al. [14] observed increased NO conversion and a decrease in the onset temperature when a potassium-containing adsorbent layer was added to a NiO-YSZ (nickel oxide-yttria stabilized zirconium oxide) or NiO-CGO based cell for electrochemical deNO<sub>x</sub>. Hamamoto et al. ascribed the increased performance to potassium's ability to adsorb NO and also saw NO decomposition when oxygen was present, which was not observed in this work. The difference could be due to the LSF15-CGO10 electrode used in this work has a larger affinity for O<sub>2</sub> reduction than the NiO-YSZ and NiO-CGO cell used by Hamamoto et al. Another explanation of the increased performance after addition of KNO<sub>3</sub> and K<sub>2</sub>O may be the K act as promoter, a phenomenon well-known from heterogeneous catalysis [29]. However based on the results in this work it is not possible to distinguish whether the KNO<sub>3</sub> and K<sub>2</sub>O mainly improves the performance by increasing the adsorption or by acting as promoters.

With respect to the results obtained in 1000 ppm NO + 10% O<sub>2</sub>, it should be noted since the current densities are similar for both the non-impregnated cell stacks and the impregnated cell stacks, but the conversion from NO to NO<sub>2</sub> is higher for the impregnated stacks, the effect of the K-species is not to generally increase the performance of the cell stacks, i.e. to increase both the O<sub>2</sub> and the NO conversion, but specifically to increase the NO conversion.

A clear observation in this work was increased NO<sub>2</sub> concentrations during polarisation at the temperature range where the largest NO conversion was observed, i.e. in the high temperature range for the non-impregnated samples and in the low temperature range for the impregnated samples. For the non-impregnated electrodes this likely show just as reduction of NO into N<sub>2</sub> on the cathodes increases with

temperature, so does the oxidation of NO into NO<sub>2</sub> on the anodes of the cell stack. One may speculate if the effect of the KNO<sub>3</sub> and K<sub>2</sub>O on the impregnated electrodes only is to act as an NO<sub>x</sub> adsorbent, or if KNO<sub>3</sub> and K<sub>2</sub>O may also facilitate the catalytic formation of NO<sub>2</sub>, thereby increasing the total NO<sub>x</sub> removal by increasing the concentration of the intermediate NO<sub>2</sub>. This is of interest since NO<sub>2</sub> has been identified as an important intermediate for electrochemical reduction of NO<sub>x</sub> by Werchmeister et al. [16, 30]. However, according to literature K-compounds are very poor in catalyzing the oxidation of NO to NO<sub>2</sub> [31]. The most likely explanation of the increased NO<sub>2</sub> level in the low temperature range for the impregnated samples is due to release of NO<sub>2</sub> during the reduction of the KNO<sub>3</sub>-storage compound, as NO<sub>x</sub> release is also observed for conventional NSR catalysts during the reduction cycle [32].

The results from the conversion measurements show at 350 °C a marked jump in the activity and the current efficiency for the impregnated cells stacks. 350 °C is above the melting point of KNO<sub>3</sub> (m.p. 334 °C [33]) and the better performance at 350 °C may for this reason be due to the presence of molten KNO<sub>3</sub>, which may increase the performance by being more mobile compared to solid KNO<sub>3</sub>. The performance decrease from 350 °C to higher temperatures may be due to the degradation phenomena which also caused the degradation of the electrode microstructure as observed on the SEM images.

#### *Effect of impregnation on serial and polarisation resistance*

The impedance spectra of the non-impregnated cell stack were fitted with the equivalent circuit  $R_s(R_1Q_1)(R_2Q_2)(R_3Q_3)$ , where R is a resistance and Q a constant phase element. For the impregnated cell stacks the same equivalent circuit was used, apart from for some spectra a fourth (RQ) element had to be included in order to obtain a satisfactory fit. Representative examples of impedance spectra and their deconvolution are shown in Fig. 8 to Fig. 10 for the three different samples.

The serial resistance ( $R_s$ ) and polarisation resistance ( $R_p$ ) obtained from the fitting are stated in Table 3. In general the serial resistances of the impregnated stacks are lower than for the non-impregnated stacks at low temperatures, but higher than for the non-impregnated stacks at higher temperatures.

A possible explanation of the lower serial resistance for the impregnated cell stacks at low temperatures could be improved sintering of the stack due to the presence of potassium [34, 35], or establishment of an easier current pathway through some part of the cell stack. The latter point follows from the conductivities of CGO being  $\approx 0.001$  S/cm at 350 °C [21] while the conductivity of the molten  $\text{KNO}_3$  at 350 °C is 0.699 S/cm [36], which means at 350 °C the reduced serial resistance observed for the  $\text{KNO}_3$  impregnated sample may be explained by the current passing through the  $\text{KNO}_3$  instead of the CGO electrolyte. Unfortunately it has despite of extensive search not been possible to find information on the conductivity of  $\text{K}_2\text{O}$  and solid  $\text{KNO}_3$  at 300 °C, for this reason it cannot be estimated here, if an alternative current path is a realistic explanation of the reduced serial resistance observed on the impregnated cell stacks at 300 °C. It is also noticed, while the serial resistance of the non-impregnated cell stacks is almost unchanged from the beginning to the end of the cell test, the serial resistance of the impregnated samples increases by a factor 8-10.

With respect to the polarisation resistance missing values in Table 3 for the impregnated samples are due to poor quality of the impedance spectra recorded at low temperatures. With one exception the polarisation resistance during the cell test is always lower on the impregnated cell stacks compared to the non-impregnated cell stack. The polarisation resistance of the  $\text{K}_2\text{O}$  impregnated sample is between 40 and 80% smaller than the polarisation resistance of the non-impregnated cell, even though from 450 °C to 500 °C the polarisation resistance of the  $\text{K}_2\text{O}$  impregnated sample starts to increase. With respect to the polarisation resistance at 300 °C after the test, the resistance of both the impregnated cell stacks is more than twice the polarisation resistance of the non-impregnated cell stack.

The impedance results are consistent with the results from the conversion measurements and the SEM images, as they show the impregnations increases the electrochemical performance of the cell stacks, but also causes severe degradation. The degradation causes the pronounced increased in  $R_s$  and  $R_p$  from the beginning to the end of the test, and is related to the breakdown of the electrode microstructure observed on the SEM images. Due to the degradation problems it was not possible to identify the processes contributing to the polarisation resistance of the impregnated cell stacks. However for the non-impregnated cell stack some of the processes could be identified, as described in the following.

#### *Electrochemical processes in the non-impregnated cell stack*

As previously mentioned, the impedance spectra recorded in 1000 ppm NO+10% O<sub>2</sub> could be fitted with the equivalent circuit  $R_s(R_1Q_1)(R_2Q_2)(R_3Q_3)$ . The process located at the highest frequency and fitted by the subcircuit ( $R_1Q_1$ ) had the activation energy 1 eV and a near-equivalent capacitance of  $2 \times 10^{-8}$  F/cm<sup>2</sup>, the near-equivalent capacitance remains constant with temperature. This process was recognized in spectra recorded in all the three different atmospheres: 1000 ppm NO + 10% O<sub>2</sub>, 1000 ppm NO and in 10% O<sub>2</sub>. The independency on the atmosphere combined with the size of the activation energy identifies the arc as belonging to intrinsic processes in the cell stack, like oxygen ion transport in the electrolyte and across the electrolyte electrode interface [37].

The process located in the middle frequency region in 1000 ppm NO + 10% O<sub>2</sub> has the activation energy 0.57 eV. The near-equivalent capacitance associated with the process increases with temperature, from  $1.7 \times 10^{-5}$  F/cm<sup>2</sup> at 300 °C to  $5.2 \times 10^{-5}$  F/cm<sup>2</sup> at 500 °C. In 10% O<sub>2</sub> the characteristics of the middle frequency arc were similar, but not totally identical to in 1000 ppm NO +10% O<sub>2</sub>. In 10% O<sub>2</sub> the arc had the activation energy 0.67 eV and the capacitance increased with temperature, but a little less steeply compared to in 1000 ppm NO +10%

O<sub>2</sub>. The fact that the middle frequency arc depends on the atmosphere indicates the arc may be related to processes like adsorption, diffusion and charge transfer at or near the triple-phase boundary (TPB) [37]. This also correlates well with the temperature dependency observed for the capacitance, as increasing temperature will increase the TPB zone and thereby increase the associated capacitance. It should be noted the activation energy in 1000 ppm NO + 10% O<sub>2</sub> is in good agreement with the activation energies reported by Werchmeister et al. for the TPB process in 1% NO on LSF/CGO electrodes [16]. In contradiction to this the activation energy 0.67 eV found in 10% O<sub>2</sub> is considerably below the activation energy observed by Werchemister et al. in air, where the activation energies was in the range 1.2-1.5 eV [16].

The process located at the lowest frequency has the activation energy 0.52 eV in 1000 ppm NO + 10% O<sub>2</sub>, and 0.20 eV in 10% O<sub>2</sub>. The large discrepancy between the two activation energies indicate this arc represent two different processes depending on whether NO is present in the atmosphere or not. The lack of temperature dependency for the process in 10% O<sub>2</sub> combined with the appearance at the lowest frequencies in the spectrum indicates this process could be related to gas phase diffusion [37]. The low frequency process when NO is present is likely not a gas phase diffusion process due to the relatively high activation energy observed. In the work by Werchmeister et al. [16] the arc observed at the lowest frequencies in NO containing atmospheres was ascribed to conversion of intermediately formed NO<sub>2</sub>. However, for this NO<sub>2</sub> conversion arc a low activation energy in the range 0.2-0.3 eV was reported, which makes it unlikely the arc observed in this work is an NO<sub>2</sub> conversion arc. The best explanation of the low frequency arc is so far it is related to one of the processes dissociative adsorption, surface diffusion and charge transfer at or near the TPB. One or more of these processes were also expected to account for the middle frequency process observed in this work. It is interesting to note the activation energies 0.57 eV and 0.52 eV found in this work for the middle and low frequency process respectively, are in good agreement with the activation energies observed by Werchmeister et al. for the TPB related processes on LSF and LSCF electrodes.



## Conclusion

In the present work the effect of  $\text{KNO}_3$  and  $\text{K}_2\text{O}$  impregnation on the  $\text{NO}_x$ -conversion on LSF15-CGO10 electrodes was investigated. In an atmosphere only containing 1000 ppm NO in Ar impregnation with  $\text{KNO}_3$  and  $\text{K}_2\text{O}$  increased the conversion of NO significantly in the temperature range 300-350 °C. Increased  $\text{NO}_2$  concentration was observed in the temperature range where the cell stacks were most active, i.e. for the impregnated cell stacks the highest  $\text{NO}_2$  concentration were observed in the low temperature range, and for the non-impregnated cell stack the highest  $\text{NO}_2$  concentrations were observed in the high temperature range.

When oxygen was present in the atmosphere together with the NO neither the non-impregnated nor the impregnated cell stacks were able to convert  $\text{NO}_x$  into  $\text{N}_2$ . However a marked difference was observed between the non-impregnated and the impregnated cell stacks in 1000 ppm NO + 10%  $\text{O}_2$ : Whereas the non-impregnated cell stack converted NO into  $\text{NO}_2$  under polarisation the impregnated cell stacks converted  $\text{NO}_2$  into NO under polarisation.

The impregnation with  $\text{KNO}_3$  and  $\text{K}_2\text{O}$  overall decreased the polarisation resistance of the cell stacks, but also introduced severe degradation problems into the stack, as breakdown of the electrode microstructure was observed. Due to the degradation it was not possible to identify the processes contributing to the polarisation resistance of the impregnated stacks. However for the non-impregnated stack oxygen-ion transport and TPB related processes were found to dominate the polarisation resistance in 1000 ppm NO +10%  $\text{O}_2$ .

Further experiments are needed to clarify, how  $\text{KNO}_3$  and  $\text{K}_2\text{O}$  impregnation affects the  $\text{NO}_x$  conversion under polarisation, among this the role of  $\text{NO}_2$  in the reaction mechanism. Also the exact cause of the increased degradation observed on impregnated samples is currently not well-understood.

## **Acknowledgements**

This work was supported by the Danish Strategic Research Council under contract no. 09-065183. Colleagues at the Fuel Cell and Solid State Chemistry Division, Technical University of Denmark, are thanked for help and fruitful discussions.

## **References**

1. Wark K, Warner CF, Davis WT (1998) Air Pollution Its Origin and Control, Third edition. Addison Wesley Longman, Inc., USA
2. Skalska K, Miller JS, Ledakowicz S (2010) Sci Total Environ 408:3976-3989
3. Stoukides M (2000) Catal Rev - Sci Eng 42:1-70
4. Bredikhin S, Hamamoto K, Fujishiro Y, Awano M (2009) Ionics 15:285-299
5. Hansen KK (2005) Appl Catal B 58:33-39
6. Pancharatnam S, Huggins RA, Mason DM (1975) J Electrochem Soc 122:869-875
7. Cicero DC, Jarr LA (1990) Sep Sci Technol 25:1455-1472
8. Hibino T (1994) Chem Lett 5 :927-930
9. Walsh KJ, Fedkiw PS (1997) Solid State Ionics 104:97-108
10. Hibino T, Ushiki K, Kuwahara Y, Mizuno M, Mazegi A, Iwahara H (1995) J Chem Soc Faraday Trans 91:
11. Hansen KK, Christensen H, Skou EM (2000) Ionics 6:340
12. Bredikhin S, Matsuda K, Maeda K, Awano M (2002) Solid State Ionics 149:327-333
13. Nagao M, Yoshii T, Hibino T, Sano M, Tomita A (2006) Electrochem Solid-State Lett 9:J1-J4
14. Hamamoto K, Fujishiro Y, Awano M (2008) J Electrochem Soc 155:E109-E111
15. Werchmeister RML, Hansen KK, Mogensen M (2010) Mater Res Bull 45:1554-1561
16. Werchmeister RML, Hansen KK, Mogensen M (2010) J Electrochem Soc 157:P107-P112
17. Hibino T, Inoue T, Sano M (2000) Solid State Ionics 130:19-29
18. Teraoka Y, Zhang HM, Okamoto K, Yamazoe N (1988) Mater Res Bull 23:51-58
19. Patrakeeve MV, Bahteeva JA, Mitberg EB, Leonidov IA, Kozhevnikov VL, Poeppelmeier KR (2003) J Solids State Chem 172:219-231
20. Ralph JM, Rossignol C, Kumar R (2003) J Electrochem Soc 150:A1518-A1522

21. Dalslet B, Blennow P, Hendriksen PV, Bonanos N, Lybye D, Mogensen M (2006) J of Solid State Electrochem 10:547-561
22. Lesage T, Saussey J, Malo S, Hervieu M, Hedouin C, Blanchard G, Daturi M (2007) Appl Catal B 72:166-177
23. Teraoka Y, Kanada K, Kagawa S (2001) Appl Catal B 34:73-78
24. Shangguan WF, Teraoka Y, Kagawa S (1998) Appl Catal B 16:149-154
25. Kaspar J, Fornasiero P, Hickey N (2003) Catal Today 77:419-449
26. Zhang Z, Zhang Y, Su Q, Wang Z, Li Q, Gao X (2010) Environ Sci Technol 44:8254-8258
27. Chick LA, Pederson LR, Maupin GD, Bates JL, Thomas LE, Exarhos GJ (1990) Mater Lett 10:6-12
28. He Z, Bohm K, Keel AL, Nygaard FB, Menon M, Hansen KK (2009) Ionics 15:427-431
29. Chorkendorff I, Niemantsverdriet JM, (2003) Concepts of Modern Catalysis and Kinetics. Wiley-VCH GmbH & Co. KGaA, Weinheim
30. Werchmeister RML, Hansen KK, Mogensen M (2010) J Electrochem Soc 157:P35-P42
31. Toops TJ, Smith DB, Partridge WP (2006) Catal Today 114:112-124
32. Epling WS, Yezerets A, Currier NW (2007) Appl Catal B 74:117-129
33. Haynes WM, Lide DR (2010-2011) CRC Handbook of Chemistry and Physics, 91st edition. Taylor and Francis Group, LCL,
34. Bruno J, Cavaleiro A, Zaghete M, Varela J (2006) Ceram Int 32:189-194
35. Nzihou A, Adhikari B, Pfeffer R (2005) Ind Eng Chem Res 44:1787-1794
36. Janz GJ (1967) Molten Salts Handbook. Academic Press Inc., New York
37. Jørgensen MJ, Mogensen M (2001) J Electrochem Soc 148:A433-A442

**Table 1** NO<sub>x</sub> conversion [%] for a non-impregnated cell stack, a KNO<sub>3</sub> impregnated cell stack and a K<sub>2</sub>O impregnated cell stack.<sup>a</sup>

Temperature [ °C]	Non-impregnated	KNO <sub>3</sub> imp.	K <sub>2</sub> O imp.
300	0	2	3
350	0	17	15
400	4	-1 *	13
450	15	3	
500	43		15

<sup>a</sup> The cell stack was supplied with 1000 ppm NO and polarised at -3V for 2h. The stated values are the percentage of NO<sub>x</sub> converted into N<sub>2</sub>.

\*-1% conversion of NO<sub>x</sub> into N<sub>2</sub> corresponds in principle to conversion of N<sub>2</sub> into NO<sub>x</sub>. But since this -1% corresponds to only 4 ppm N<sub>2</sub>, it is considered to be within the general uncertainty of the experiment.

**Table 2** Current efficiency [%] for a non-impregnated cell stack, a KNO<sub>3</sub> impregnated cell stack and a K<sub>2</sub>O impregnated cell stack.<sup>a</sup>

Temperature [ °C]	Non-impregnated	KNO <sub>3</sub> imp.	K <sub>2</sub> O imp.
300	0	8	38
350	0	59	73
400	5	-8	37
450	10	4	
500	11		15

<sup>a</sup> The current efficiency is calculated according to Eq.(5). The cell stack was supplied with 1000 ppm NO in Ar and polarised at -3V for 2 h.

**Table 3** Serial resistance ( $R_s$ ) and polarisation resistance ( $R_p$ ) for three LSF15-CGO10 porous cell stacks without impregnation (“non-impregnated”), with  $\text{KNO}_3$  impregnation and with  $\text{K}_2\text{O}$  impregnation.<sup>a</sup>

Temp. [°C]	<u><math>R_s</math> [<math>\Omega\text{cm}^2</math>]</u>			<u><math>R_p</math> [<math>\Omega\text{cm}^2</math>]</u>		
	Non-imp.	$\text{KNO}_3$ imp.	$\text{K}_2\text{O}$ imp.	Non-imp.	$\text{KNO}_3$ imp.	$\text{K}_2\text{O}$ imp.
300	140	110	100	5700		
350	47	110	31	3200		1700
400	19	64	20	1700	4300	630
450	11	110	16	920	780	190
500	8	40	15	420	210	250
300(post) <sup>b</sup>	140	810	1000	9700	24000	23000

<sup>a</sup> The cell stacks were supplied with 1000 ppm NO + 10%  $\text{O}_2$  while the EIS spectra were recorded.

<sup>b</sup> 300(post) refers to the impedance spectra recorded at the end of the experiment, i.e. after temperature variations and polarisation experiments had been performed.

**Fig. 1** Cross-section of a non-impregnated LSF15-CGO10 cell stack. The six light grey layers are porous LSF15-CGO10 electrode layers, the 5 dark grey layers are porous CGO10 electrolyte layers and on each side of the cell stack the porous Au current collector is observed (only marked on the top side)

**Fig. 2** Sketch of set-up for testing of porous cell stacks (reprinted with permission from [15])

**Fig. 3** Microstructure of the electrode of a) a non-impregnated LSF15-CGO10 cell stack, b) cell stack impregnated with  $\text{KNO}_3$  and c) cell stack impregnated with  $\text{KNO}_3$  and subsequently heated to 700 °C to decompose the  $\text{KNO}_3$  into  $\text{K}_2\text{O}$ . White arrows point at impregnated  $\text{KNO}_3$  and black arrows on  $\text{K}_2\text{O}$

**Fig. 4** Outer electrode of  $\text{KNO}_3$  impregnated cell stack a) before electrochemical cell testing and b) after electrochemical cell testing

**Fig. 5** Conversion of NO into  $\text{NO}_2$  relative to the  $\text{NO}_x$  concentration before polarisation in 1000 ppm NO. The cell stacks were polarized at 3 V for 2 h and the stacks were supplied with 1000 ppm NO in Ar. The dashed lines are for visual guidance only

**Fig. 6** Relative conversion of NO during 2 h polarisation at 3 V on non-impregnated and impregnated LSF cell stacks. Positive values correspond to formation of NO and negative values to removal of NO. The dashed lines are for visual guidance only

**Fig. 7** Relative conversion of  $\text{NO}_2$  during 2 h polarisation at 3 V on non-impregnated and impregnated LSF cell stacks. Positive values correspond to formation of  $\text{NO}_2$  and negative values to removal of  $\text{NO}_2$ . The dashed lines are for visual guidance only

**Fig. 8** Impedance spectrum recorded in 1000 ppm NO + 10%  $\text{O}_2$  at 400 °C on non-impregnated cell stack. The solid line represents the deconvolution of the entire spectrum and the dashed lines the deconvolution of the individual processes. For solid points the frequency of the data point is stated

**Fig. 9** Impedance spectrum recorded in 1000 ppm NO + 10%  $\text{O}_2$  at 400 °C on  $\text{KNO}_3$  impregnated cell stack. The solid line represents the deconvolution of the entire spectrum and the dashed lines the deconvolution of the individual processes. For solid points the frequency of the data point is stated



**Fig. 10** Impedance spectrum recorded in 1000 ppm NO + 10% O<sub>2</sub> at 400 °C on K<sub>2</sub>O impregnated cell stack. The solid line represents the deconvolution of the entire spectrum and the dashed lines the deconvolution of the individual processes. For solid points the frequency of the data point is stated

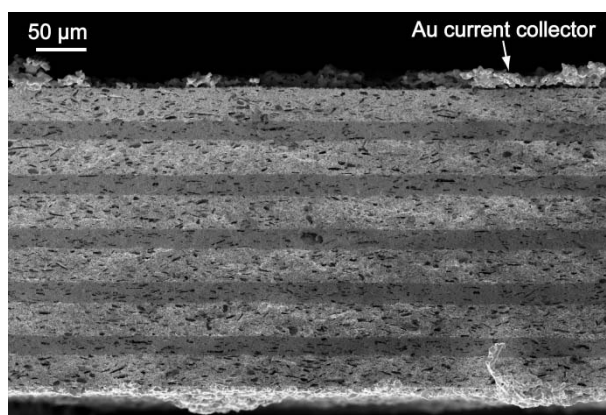


Fig.1

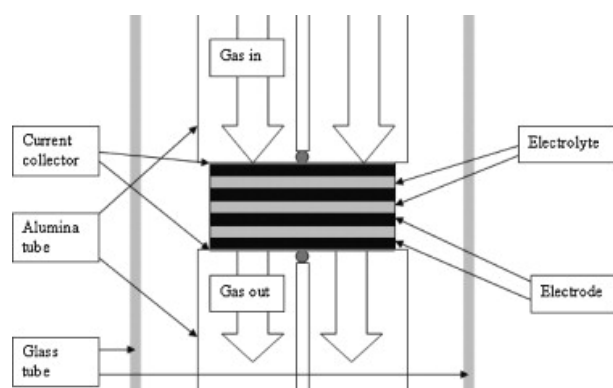


Fig. 2

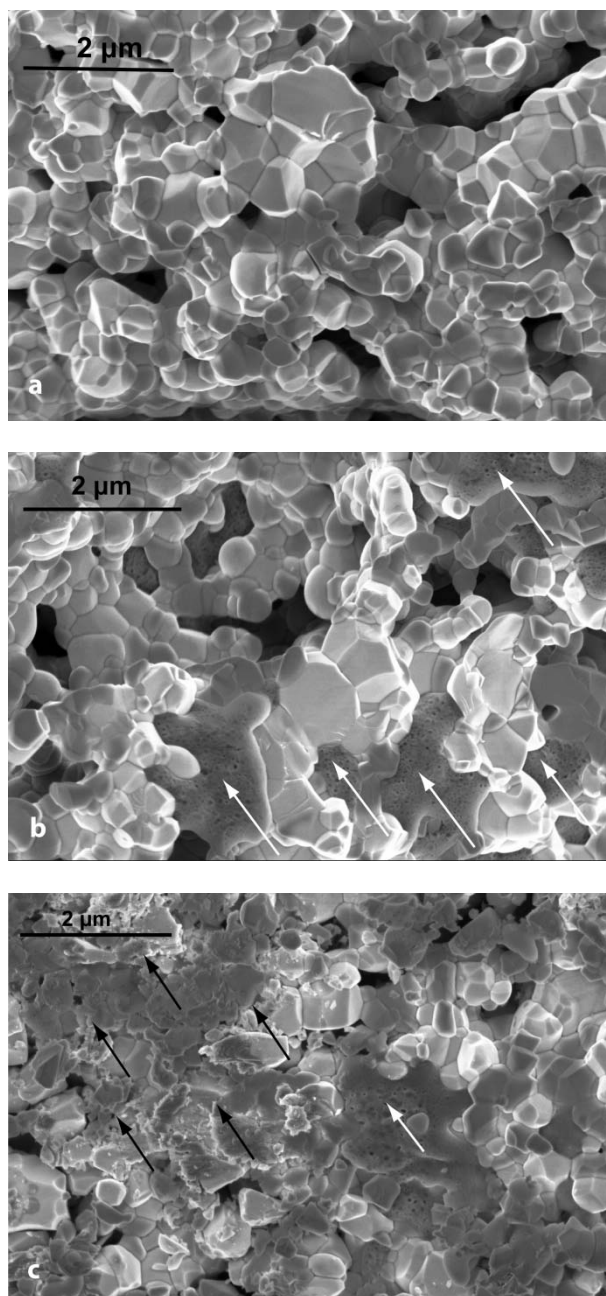


Fig. 3

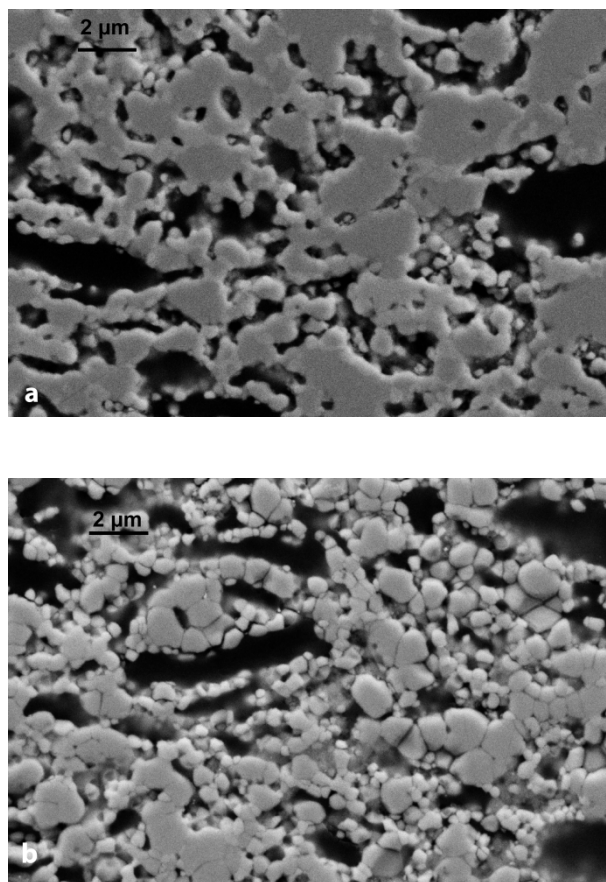


Fig. 4

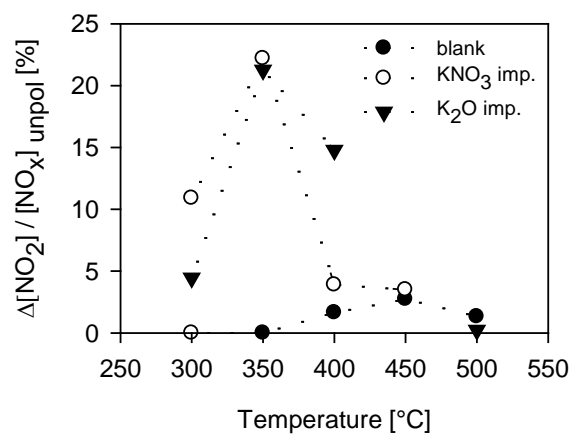


Fig. 5

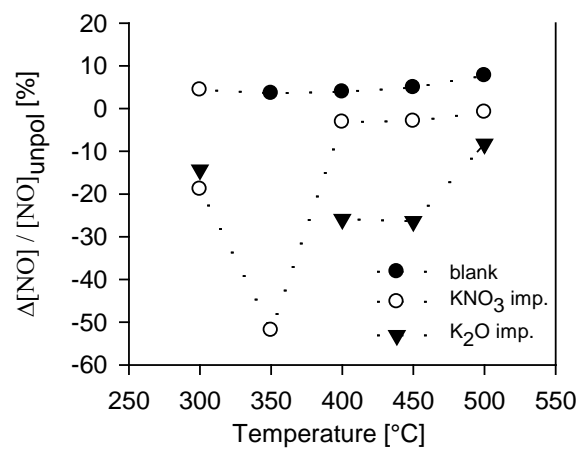


Fig. 6

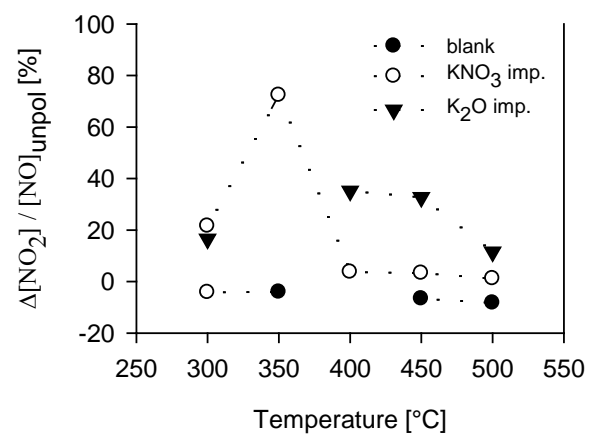


Fig. 7



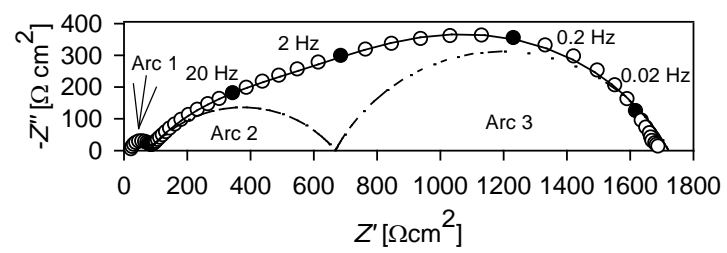


Fig. 8

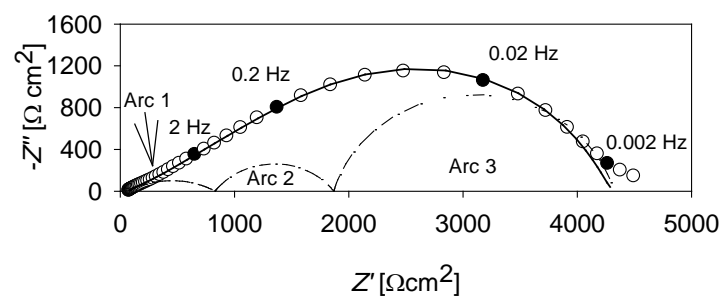


Fig. 9

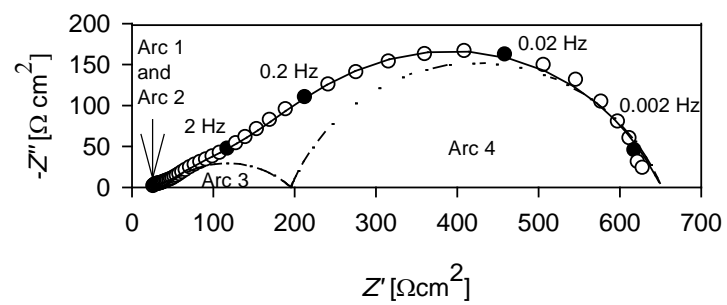


Fig. 10